

Scaling of Energy Barriers for Flux Lines and Other Random Systems

Barbara Drossel and Mehran Kardar

Department of Physics, Massachusetts Institute of Technology, Cambridge, Massachusetts 02139

(April 1, 2018)

Using a combination of analytic arguments and numerical simulations, we determine lower and upper bounds for the energy barriers to the motion of a defect line in a random potential at low temperatures. We study the cases of magnetic flux lines in high- T_c superconductors in 2 and 3 dimensions, and of domain walls in 2 dimensional random-field Ising models. The results show that, under fairly general conditions, energy barriers have the same scaling as the fluctuations in free energy, except for possible logarithmic factors. This holds not only for barriers between optimal configurations of the line, but also for barriers separating any metastable configuration from a configuration of minimal energy. Similar arguments may be applicable to other elastic media with impurities, such as bunches of flux lines.

I. INTRODUCTION

Directed paths in random media (DPRM) [1] are simple realizations of glassy systems [2,3]. Some examples are pinned flux lines (FL) in high- T_c superconductors, and domain walls in random field and random bond Ising models. In thermal equilibrium, a magnetic FL is pinned by defects (oxygen impurities, grain boundaries, etc.) in the superconductor which lower its energy [4]. The resulting elastic distortions are limited by the line tension which opposes the bending of the line. This competition leads to a free energy landscape for the FL which is rather complicated and has many local minima, i.e. metastable states [5]. When an electric current flows through the system, the FL feels a Lorentz force perpendicular to its orientation and to the current direction. As long as the current is not strong enough to overcome the pinning forces, the line moves by thermally activated jumps of line segments between metastable configurations [6–8]. The length of these line segments is estimated by the condition that the free energy barrier for a jump should be of the same order as the gain in free energy due to that jump. These dynamics are believed to be the reason for the nonlinear voltage-current characteristics found in experiments [4].

Randomly placed impurities in Ising ferromagnets may generate either a random magnetic field or random exchange couplings [9]. The free energy landscape for domain walls in these systems is determined by the competition between the pinning energy and the energy cost (per unit length or area) for creating the wall. When the system is quenched to a low temperature, the magnetic domains grow. As for the flux line, the free energy gain due to the motion of a domain wall segment is expected to be of the same order as the free energy barrier which has to be overcome.

Since energy barriers play an important role in the dynamics of glassy systems, it is essential to know their properties. The scale of these barriers should grow with observation size L like a power law L^ψ . Usually, it is

assumed that the only energy scale in the system is set by the fluctuations in free energy which increase as L^θ , and that therefore $\psi = \theta$ [9,8]. However, it is also quite possible that the heights of the ridges in the random energy landscape scale differently from those of the valleys that they separate, with $\psi > \theta$. Yet another scenario is that transport occurs mainly along a percolating channel of exceptionally low energy valleys with $\psi < \theta$.

A first attempt to clarify this situation was taken in Ref. [10], where $\psi = \theta$ was established for a FL moving in 2 dimensions. Using a combination of analytic arguments and numerical simulations, lower and upper bounds to the barrier were found. This argument was then extended to a FL in 3 dimensions [11], yielding again $\psi = \theta$. In this article, we present in more detail the arguments discussed briefly in these earlier papers, including also systems with long-range correlated randomness (random-field Ising models) in 2 dimensions. We obtain in all cases lower and upper bounds to the barrier that scale as L^θ , except for possible logarithmic factors, leading to $\psi = \theta$. Furthermore, it is argued that the result $\psi = \theta$ holds also in higher dimensions, as long as the distribution of minimal energies decays exponentially. In all cases, the line can move through the system by encountering energy fluctuations of only order L^θ around the mean minimal energy. We also show that a line which initially has a larger energy can reach this region of minimal energies by crossing barriers of order L^θ (or smaller).

The outline of the paper is as follows: In section II, we determine the energy barrier for a FL moving in 2 dimensions. In section III, we apply the same algorithm to determine the energy barrier to the motion of domain walls in 2-dimensional random-field Ising systems. In section IV, we study energy barriers for a FL in 3 dimensions and discuss also the behavior in higher dimensions. In section V, we take a general look at the energy landscape and show that a line can move from any initial configuration to a minimal configuration by going over no barrier higher than L^θ . In section VI, we try to put the definition of energy barriers on a more solid foundation, and

section VII argues that the results of the paper can be generalized to other elastic media with impurities.

II. ENERGY BARRIERS FOR FLUX LINES IN 2 DIMENSIONS

In two dimensions, we represent a DPRM by the following model: The line is discretized to lie on the bonds of a square lattice, directed along its diagonal. Each segment of the line can proceed along one of two directions, leading to a total of 2^t configurations after t steps. These configurations are labelled by the set of integers $\{x(\tau)\}$ for $\tau = 0, 1, \dots, t$, giving the transverse coordinate of the line at each step (clearly constrained such that $x(\tau + 1) = x(\tau) \pm 1$). To each bond on the lattice is assigned a (quenched) random energy equally distributed between 0 and 1. The energy of each configuration is the sum of all random bond energies on the line. Without loss of generality, we set $x(0) = 0$.

Some exact results are known for this model [1]: The fluctuations in the free energy at finite temperature scale as $t^{1/3}$. The meanderings of the transverse coordinate of the line scale as t^ζ , where $\zeta = 2/3$ is the roughness exponent. The scaling behavior of the pinned FL is governed by a zero-temperature fixed point [9] where energy fluctuations scale in the same way. A FL at low temperatures, and in thermal equilibrium, is likely to spend most of the time in configurations of minimal energy. For each endpoint (t, x) with $x = -t, -t + 2, \dots, t$, there is a configuration of minimal energy $E_{min}(x|t)$ which can be obtained numerically in a time of order t^2 . It is known that for $|x| < x_c \propto t^{2/3}$, the function $E_{min}(x|t)$ behaves as a random walk and is thus asymptotically Gaussian distributed [1,12]. Since beyond the interval $[-x_c, x_c]$ the energy of minimal paths is systematically larger, we consider in this paper only the region $[-x_c, x_c]$. Fig.1 shows minimal paths of length $t = 256$ to endpoints between $x = -96$ and $x = +96$.

We want to find the energy barrier that has to be overcome when the line is moved from an initial minimal energy configuration $\{x_i(\tau)\}$ between $(0, 0)$ and $(t, -x_f)$ to a final configuration $\{x_f(\tau)\}$ between $(0, 0)$ and $(t, +x_f)$, with $x_f \equiv x_f(t) \leq x_c$. The only elementary move allowed is flipping a kink along the line from one side to the other (except at the end point). Thus the point (τ, x) can be shifted to $(\tau, x \pm 2)$. Each route from the initial to the final configuration is obtained by a sequence of such elementary moves. For each sequence, there is an intermediate configuration of maximum energy, and a barrier which is the difference between this maximum and the initial energy. In a system at temperature T , the probability that the FL chooses a sequence which crosses a barrier of height E_B is proportional to $\exp(-E_B/T)$, multiplied by the number of such sequences. We assume that, as is the case for the equilibrium DPRM, the ‘‘entropic’’ factor of the number of paths does not modify scaling

behavior. Thus at sufficiently low temperatures, the FL chooses the optimal sequence which has to overcome the least energy, and the overall barrier is the minimum of barrier energies of all sequences.

Since the number of elementary moves scales roughly as the area between the initial and final lines, the number of possible sequences grows as t^{x_t} . This exponential growth makes it practically impossible to find the barrier by examining all possible sequences, hampering a systematic examination of barrier energies. Rather than finding the true barrier energy, we proceed by placing upper and lower bounds on it.

The lower bound was given in Ref. [13], and is obtained as follows: The endpoint of the path has to visit all sites (t, x) with $|x| \leq x_f$, and the energy of any path ending at (t, x) is at least as large as $E_{min}(x|t)$. Therefore the barrier energy cannot be smaller than $\max[E_{min}(x|t) - E_{min}(-x_f|t)]$ for $x \in [-x_f, x_f]$. When x_f is sufficiently small, the probability distribution of this lower bound is identical to that of the maximal deviation of a random walk of length x_f [14]. The latter is a Gaussian distribution with a mean value proportional to $\sqrt{x_f}$, and a variance scaling as x_f . This growth saturates for x_f of the order of $t^{2/3}$, leading to the scaling behaviors,

$$\begin{aligned} \langle E_-^{(sr)}(t, x) \rangle &= t^{1/3} f_1^{(sr)}(x/t^{2/3}), & \text{and} \\ \text{var}(E_-^{(sr)}) &= t^{2/3} f_2^{(sr)}(x/t^{2/3}), \end{aligned} \quad (1)$$

for the lower bound and its variance. The functions $f_1^{(sr)}(y)$ and $f_2^{(sr)}(y)$ are proportional to \sqrt{y} and y for small y , respectively, and go to a constant for $y = O(1)$. Our simulation results for systems with $t = 256, 512, 1024, 2048, \text{ and } 4096$ confirm this expectation. Fig.2 shows the scaling functions $f_1^{(sr)}(y)$ and $f_2^{(sr)}(y)$ for different t , and the collapse is quite satisfactory. However, the initial growth proportional to $\sqrt{x_f}$, is not clearly seen at these sizes.

To obtain an upper bound for the barrier, we specify an explicit algorithm for moving the line from its initial to final configuration. This is achieved by finding a sequence of intermediate steps. It is certainly advantageous to keep the intermediate paths as close to minimal configurations as possible. We therefore proceed in the following way: We first find the minimal paths connecting $(0, 0)$ to the points $(t-1, x)$ with $x_i(t-1) < x < x_f(t-1)$, and we add a last step to the left (from $(t-1, x)$ to $(t, x-1)$). If $x_i(t-1) > x_i(t) = -x_f$, we then move the point $(t, -x_f)$ to $(t, -x_f + 2)$. Now the path has the same endpoint as the first intermediate minimal path. We then move the path to this first intermediate configuration (the precise prescription will be given below), and then we move again the endpoint. This procedure is repeated, until the path reaches its final configuration. At each step, we obtain a local barrier path which separates two neighboring minimal configurations. The overall barrier is of course the one with the highest energy. While it may occasionally be possible to go to the next intermediate configuration

in a single elementary move (as defined above), this is generally not the case. Intermediate minimal paths with the same endpoint may be quite far apart at coordinates $\tau < t$. The reason is simple: suppose the random potential has a large positive fluctuation, a “mountain.” The minimal energy paths will then circumvent this region by going to its right or left. The last path going to the left and the first one going to the right have almost the same energy. They form a loop which can be quite large and is likely to enclose the barrier when both paths separate already at small τ . Such loops have been conjectured [8,7] to play an important role in the low-temperature dynamics of the DPRM. Since the transverse fluctuations of a minimal path of length t grow as $t^{2/3}$, we expect the lateral size of these loops to also be of this order.

The algorithm for moving a line of length $t = 2^n$ from an intermediate configuration $\{x_1(\tau)\}$ to another one $\{x_2(\tau)\}$, with $x_2(t) = x_1(t)$ is as follows: If $x_2(\tau) \leq x_1(\tau) + 2$ for all τ , we can choose a sequence of elementary moves such that at most two bonds of the line are not on one or the other minimal path, leading to a barrier of order 1 between the two. If $x_2(\tau) > x_1(\tau) + 2$ for some τ , the two paths enclose a loop. We then consider the points $(t/2 - 1, x)$ with $x_1(t/2 - 1) < x < x_2(t/2 - 1)$. For each of these points, we find a minimal segment of length $t/2 - 1$, connecting the point $(t/2 - 1, x)$ to $(0, 0)$ by a minimal path, and we take a final step to the left from $(t/2 - 1, x)$ to $(t/2, x - 1)$. In the same way, we connect the points $(t/2 + 1, x)$ with $x_1(t/2 + 1) < x < x_2(t/2 + 1)$ to $x_1(t)$ via minimal paths and add a first step to the right from $(t/2, x - 1)$ to $(t/2, x)$. Two such segments form together an almost minimal path of length t , constrained to go through intermediate points at $t/2$ and $t/2 \pm 1$. We next move the line $\{x_1(\tau)\}$ stepwise through this sequence of almost minimal paths. If $x_i(t/2 - 1) = x_i(t/2) - 1$, we first move the upper segment. If $x_i(t/2) = x_i(t/2 + 1) + 1$, we then move the lower segment. Then we move the midpoint. We continue by repeatedly moving the upper segment, the lower segment, and the middle point, until the final configuration $\{x_2(\tau)\}$ is reached. (If the length of the line is different from 2^n , we might have to choose the upper segment to be larger by 1 than the lower segment, or vice versa.)

The prescription for moving the segments of length $t/2$ is exactly the same as for paths of length t : If the distance between two consecutive configurations is larger than 2 for some $\tau \in [0, t/2]$, we consider the points at $(t/4 \pm 1, x)$ in between the two, and find minimal paths of length $t/4 - 1$ connecting them to the initial and final points, and add a step to the middle points. Next we attempt to move segments of length $t/2$ by repeatedly moving line portions of length $t/4$. In some cases, when the energy barrier is large, it is necessary to proceed with this construction until the cutoff scale of $t/2^{n-1} = 2$ is reached. Thus, at each intermediate configuration, the line is composed of one segment of length $t/2$, one of length $t/4$, etc; ending with two smallest pieces of length $t/2^m$ (equal to 2 in the worst case). The barrier path is

the intermediate configuration with highest energy. Fig.1 shows the barrier paths resulting from the above construction.

We now estimate the barrier energy resulting from the above construction. Each intermediate path is composed of segments of minimal paths with constrained endpoints, and we would like to find the probability distribution for the highest energy. Constraining the endpoints of a minimal path of length τ typically increases its energy by $E_-^{(sr)}(\tau) \propto \tau^{1/3}$. A subset of these intermediate paths (those that cross the largest mountains) have constraints imposed on segments of length $t, t/2, t/4$, and all the way down to unity. The number of paths in this subset (henceforth referred to as candidate barriers) grows as $N_c(t) \propto t^\alpha$, with $1 < \alpha < 1 + 2/3$. The lower limit comes from noting that for each loop of size 2^m there exist at least two loops of size 2^{m-1} , one in the upper and one in the lower half of the parent loop, thus $N_c \geq t$. The upper limit comes from the total number of intermediate configurations that grows as tx_f . The energy of each candidate barrier path is obtained in a manner similar to that of the lower bound: Instead of finding the maximum of a random walk of length $x_f \propto t^{2/3}$, we now have to examine the sum of the maxima for a sequence of shorter and shorter random walks added together. The mean value of this sum is related to the convergent series,

$$\begin{aligned} \langle E_c^{(sr)}(t) \rangle &= \\ &= \langle E_-^{(sr)}(t) + 2 E_-^{(sr)}(t/2) + 2 E_-^{(sr)}(t/4) + \dots \rangle + A \ln(t) \\ &= \langle E_-^{(sr)}(t) \rangle \left(1 + 2(2^{-1/3} + 2^{-2/3} + \dots) \right) + A \ln(t) + B \\ &\simeq \langle E_-^{(sr)}(t) \rangle \left(-1 + 2(1 - 2^{-1/3})^{-1} \right) + A \ln(t) + B \\ &= 8.69\dots \langle E_-^{(sr)}(t) \rangle + A \ln(t) + B. \end{aligned} \quad (2)$$

The correction term $A \ln(t)$, is explained as follows: Each segment of length 2^m is composed of a minimal path of length $2^m - 1$ and one step which has a random energy (the final or initial step, depending on whether the segment lies in the upper or lower half of a loop). So the energy of the segment is equal to the energy $E_-^{(sr)}(2^m)$ of a minimal path of length 2^m , plus a constant of order 1. Since a candidate barrier has $n = \ln(t)/\ln(2)$ segments, these constants add up to $A \ln(t)$, with A of the order of unity. The constant B in Eq.(2) accounts for the breakdown of the scaling form of the energy increase for small loops. The mean angle of the smallest loops (of size 2) approaches the 45° limit; their mean energy growing as $0.5t_m$. For the larger loops, the angle $t_m^{2/3}/t_m$ is small and the energy is $0.23t_m$. A finite value of m acts as a cutoff separating the two limits. The energy difference per unit length between small and large paths then leads to the additive constant B (of the order of unity) in Eq.(2).

The barrier energy is the maximum of the $N_c(t)$ energies of all candidate barriers. To find its characteristics,

we need the whole probability distribution for the energy $E_c^{(sr)}(t)$. Since $E_c^{(sr)}$ is the sum of energies coming from its minimal segments, the simplest assumption is to regard the segment energies as independent, approximately Gaussian, random variables. We then conclude that $E_c^{(sr)}(t)$ is also Gaussian distributed with a variance,

$$\begin{aligned} & \text{var} \left(E_c^{(sr)}(t) \right) \\ &= \text{var} \left(E_-^{(sr)}(t) \right) + 2 \left(\text{var} \left(E_-^{(sr)}(t/2) \right) + \dots \right) \\ &\simeq 4.40 \dots \text{var} \left(E_-^{(sr)}(t) \right) \propto t^{2/3}. \end{aligned} \quad (3)$$

Since the different segments are in fact constructed through a specific recursive procedure, their independence cannot be justified. In the worst case that they are completely dependent, the right-hand side of Eq.(3) has to be multiplied by $n = \log_2(t)$. Since our numerical results show no evidence for such a logarithmic factor, we shall not consider it any further.

It can be checked easily that (for large N), the maximum of N independent Gaussian variables of mean a and variance σ^2 , is a Gaussian of mean $a + \sigma\sqrt{2 \ln N}$ and variance $\sigma^2/(2 \ln N)$ [15]. Since the $N_c(t)$ candidate barriers have large segments in common, their energies are not independent. We can approximately take this into account by assuming a subset of them as independent, leading to $N \propto t^{\alpha'}$ for some $\alpha' < \alpha$. We thus obtain the following estimates for the mean upper bound in barrier energy,

$$\begin{aligned} \left\langle E_+^{(sr)}(x, t) \right\rangle &= \left\langle E_c^{(sr)}(x, t) \right\rangle + \sqrt{2 \ln N \text{var} E_c^{(sr)}(x, t)} \\ &\simeq \left(1 + \beta^{(sr)} \sqrt{\ln t} \right) t^{1/3} g_1^{(sr)}(x/t^{2/3}), \end{aligned} \quad (4)$$

and its variance,

$$\begin{aligned} \text{var} \left(E_+^{(sr)}(x, t) \right) &= \frac{\text{var} \left(E_c^{(sr)}(x, t) \right)}{2 \ln N^{(sr)}} \\ &\simeq \frac{t^{2/3}}{\ln t} g_2^{(sr)}(x/t^{2/3}). \end{aligned} \quad (5)$$

The functions $g_1^{(sr)}(y)$ and $g_2^{(sr)}(y)$ are proportional to \sqrt{y} and y respectively, for small y , constant at large y , and in general different from those of the lower bound.

Our numerical simulations indeed confirm the above scaling forms. The scaling functions $g_1^{(sr)}(y)$ and $g_2^{(sr)}(y)$ are plotted in Fig.2 for different values of t , after averaging over 2000 realizations of randomness. The $\sqrt{\ln(t)}$ factors are essential, as a comparable collapse is not obtained without them. In fact, the best fit to $\langle E_+^{(sr)}(t) \rangle$ is obtained by including the correction to scaling term $\propto \langle E_-^{(sr)}(t) \rangle$, and with $\beta^{(sr)} = 1$. The numerics therefore support the neglect of correlations, and the assumption of a Gaussian distributed $E_c^{(sr)}(t)$. As in the lower bound, the initial scaling proportional to $\sqrt{x_f}$ is

not clearly seen for the sizes studied. Since the leading power for the scaling of the lower and upper bounds is identical, we conclude that the barrier energies also grow as $t^{1/3}$. (It remains to be seen if the logarithmic factors are truly present, or merely an artifact of our algorithm.)

III. ENERGY BARRIERS FOR DOMAIN WALLS IN 2-DIMENSIONAL RANDOM FIELD ISING SYSTEMS

In the previous section, we considered random bond energies which were uncorrelated. The analytic argument for the upper bound relied on the random-walk behavior of $E_{min}(x|t)$ in this situation. Thus, the proof for $\psi = \theta$ can not directly be extended to other situations, where the distribution of lower bound energies is not known. An important example is the case of domain walls in 2-dimensional random-field Ising magnets. The energy for creating a domain wall is equal to the cost of flipping all spins on one side of the interface; in turn proportional to the sum of all random fields on the flipped spins. There are consequently long-range correlations in the domain wall energy in the direction perpendicular to the orientation of the wall [16].

We describe the configurations of the domain wall by essentially the same model as the FL, but assigning to each bond a random energy with long-range correlations in the x -direction. These correlations are generated by first selecting for each time t , random numbers $\{r_t^{(-N)}, r_t^{(-N+1)}, \dots, r_t^{(N-3)}, r_t^{(N-1)}\}$ equally distributed between -1 and 1 , where N is (at least) as large as the largest time occurring in the simulations. To each bond connecting (t, x) to $(t+1, x \pm 1)$ we then assign the energy

$$\frac{1}{\sqrt{2N}} \left(\sum_{i=-N}^{x-1/2 \pm 1/2} r_t^i - \sum_{x+1/2 \pm 1/2}^{N-1} r_t^i \right).$$

Fig.3 shows minimal paths of length $t = 128$. Due to the correlations, neighboring bonds have almost the same energy, and therefore minimal paths tend to have large parallel portions. Fig.4 shows the minimal energy as function of the endpoint position for a given realization of randomness, and for $t = 1024$. This curve is much smoother and has longer correlations than the corresponding curve in the case of short-range correlated randomness, where the minimal energy performs a random walk.

The fluctuations in free energy of a line are known to scale as t , and the roughness exponent is $\zeta = 1$ [17]. We determined numerically the distribution function for the minimal energy shown in Fig.5. It is very close to a Gaussian, with no apparent power-law tails. We will show that, due to this property of the minimal energy distribution, the lower and upper bounds to the barrier scale in the same way as the fluctuations in minimal energy.

As in the previous section, we move the line from an initial minimal energy configuration $\{x_i(\tau)\}$ between $(0,0)$ and $(t, -x_f)$, to a final configuration $\{x_f(\tau)\}$ between $(0,0)$ and (t, x_f) . Since the endpoint of the path has to visit all sites (t, x) with $|x| \leq x_f$, and since the energy of any path ending at (t, x) is at least as large as $E_{min}(x|t)$, the barrier energy cannot be smaller than $\max[E_{min}(x|t) - E_{min}(-x_f|t)]$. Since the distribution of minimal energies decays exponentially and has no power-law tails, we can expect that the lower bound scales in the same way as the fluctuation of the minimal energy, leading to

$$\begin{aligned} \langle E_-^{(lr)}(t, x) \rangle &= t f_1^{(lr)}(x/t), & \text{and} \\ \text{var}(E_-^{(lr)}) &= t^2 f_2^{(lr)}(x/t), \end{aligned} \quad (6)$$

for the lower bound and its variance. Our simulation results for systems with $t = 256, 512, 1024$ and 2048 confirm this expectation. Fig.6 shows the scaling functions $f_1^{(lr)}(y)$ and $f_2^{(lr)}(y)$ for different t , and the collapse is quite satisfactory. However, the initial growth proportional to x_f , is not clearly seen at these sizes. Fig.7 shows the distribution of lower bound energies. It is very close to a (half)-Gaussian of width proportional to t .

An upper bound can be obtained by exactly the same algorithm as before. The analytic argument made in the previous section, however, cannot be directly repeated, since the function $E_{min}(x|t)$ is no longer a random walk in x , and since we do not have analytic results for the lower bound. We can, however, combine analytic arguments with the numerical results for the lower bound to predict the scaling behavior of the upper bound. Since the line is always composed of minimal segments, the energy of a candidate barrier which has segments of all lengths down to the cutoff is given by

$$\begin{aligned} &\langle E_c^{(lr)}(t) \rangle \\ &= \langle E_-^{(lr)}(t) + 2 \left(E_-^{(lr)}(t/2) + E_-^{(lr)}(t/4) + \dots \right) \rangle \\ &\simeq 3 \langle E_-^{(lr)}(t) \rangle + A' \ln(t) + B'. \end{aligned} \quad (7)$$

The origin of the terms $A' \ln(t) + B'$ has been explained in the previous section (see paragraph after Eq.(2)). Since the energy distribution of the lower bound is approximately (half)-Gaussian, the energy distribution of the candidate barriers decays also like a Gaussian. The upper bound to the barrier energy is the maximum of the energies of all candidate barriers. In our simulations, we find no evidence for logarithmic factors, indicating that the number of candidate barriers increases either very slowly, or not at all, with t . From Fig.3 we can see that there is essentially one large loop over a distance of the order of the length of the path, leading to only few independent candidate barriers. As in the previous section, we find that the maximum of these candidate barriers, which is the upper bound to the barrier energy, scales in the same way as the lower bound, i.e.

$$\begin{aligned} \langle E_+^{(lr)}(x, t) \rangle &= \langle E_c^{(lr)}(x, t) \rangle + \sqrt{2 \ln N^{(lr)} \text{var} E_c^{(lr)}(x, t)} \\ &\simeq t g_1^{(lr)}(x/t), \end{aligned} \quad (8)$$

and its variance scales as

$$\begin{aligned} \text{var} \left(E_+^{(lr)}(x, t) \right) &= \text{var} \left(E_c^{(lr)}(x, t) \right) / 2 \ln N^{(lr)} \\ &\simeq t^2 g_2^{(lr)}(x/t). \end{aligned} \quad (9)$$

Fig.6 shows the scaling functions $f_2^{(lr)}$ and $g_2^{(lr)}$.

To summarize the results so far, we have established the relation $\psi = \theta$ for lines in 2-dimensional systems with short- and long-range correlated randomness. Since the considerations for both systems rely strongly on the dimensionality, it is of importance to look also at a 3-dimensional system, which is physically more relevant.

IV. ENERGY BARRIERS FOR A FLUX LINE IN 3 DIMENSIONS

In a two-dimensional system, the endpoint of the FL has to move through all points (x, t) with $x_i < x < x_f$. This property was essential for the derivation of the lower bound in the previous sections. A FL which moves in three dimensions can avoid regions in space which are energetically unfavorable for some of its segments, and one may therefore speculate that $\psi < \theta$. In this section, we first determine numerically a lower bound for the barrier energy which scales in the same way as the energy fluctuations, thus ruling out $\psi < \theta$. Further numerical results predict that an upper bound scales in the same way, thus leading to $\psi = \theta$.

The line now lies on the bonds of a cubic lattice, starting at the origin and directed along its $(1,1,1)$ diagonal. Each segment of the line can proceed in the positive direction along one of the three axes, leading to a total of 3^t configurations after t steps, with endpoints lying in the plane which is spanned by the points $(t, 0, 0)$, $(0, t, 0)$, and $(0, 0, t)$. A given configuration of the FL is labelled by vectors $\{\vec{x}(\tau)\}$ for $\tau = 0, 1, \dots, t$, giving the transverse coordinates of the FL at each step. The points $\{\vec{x}(\tau)\}$ lie on the vertices of a triangular lattice. For a given value of τ , they lie on one of three alternating sublattices.

The minimal energy $E_{min}(\vec{x}|t)$ can be obtained numerically in a time of order t^3 . The fluctuations in minimal energy are known to scale as t^θ with $\theta \simeq 0.24$, and the roughness exponent for minimal paths is $\zeta \simeq 0.62$ [18,19]. The endpoints of the minimal paths with the lowest energy lie within a distance proportional to t^ζ from the origin. Figure 8 shows the minimal energies of paths of length $t = 288$ to endpoints \vec{x} with $|\vec{x}| < O(t^\zeta)$. The highest energy in this region is represented in white, the smallest energy in black. The minimal energies are correlated over a distance of the order of t^ζ . The distribution

of minimal energies is close to a Gaussian and is shown in Fig.9. Similar to a 2-dimensional system [20] (see also Fig.5), this distribution seems to have a third cumulant since it is not completely symmetric.

A lower bound to the barrier energy is obtained as follows: While the line moves from its initial to final configuration, the transverse coordinates of its endpoint move between nearest-neighbor positions on one of the above mentioned triangular sublattices. When the endpoint is at a position \vec{x} , the energy of the line is at least as large as the minimal energy $E_{min}(\vec{x}|t)$. The maximum of all these minimal energies along the trajectory of the endpoint, minus the energy of the initial configuration, certainly bounds the barrier energy from below. Since we do not know the actual trajectory of the endpoint, we have to look for the trajectory with the smallest maximal energy. Only in this way can we be sure that we have indeed found a lower bound. This situation is fundamentally different from a 2-dimensional system, where there is only one possible trajectory for the endpoint.

Provided that the minimal energies $E_{min}(\vec{x}|t)$ are known, this lower bound is determined in polynomial time by using a transfer-matrix method: We start by assigning to the initial point \vec{x}_i a ‘‘barrier energy’’ $B(\vec{x}_i) = 0$, and to all other sites \vec{x} on the same sublattice a barrier energy $B(\vec{x}) = t$, which is certainly larger than the lower bound resulting from the algorithm after many iterations. At each step, the energy B of all sites \vec{x} , except for the initial site, is updated according to the following rule: Look for the minimum of the energies $B(\vec{x} \pm \vec{e}_i)$ of the 6 neighbors. If this is smaller than $B(\vec{x})$, replace $B(\vec{x})$ by this minimum, or by $E_{min}(\vec{x}|t) - E_{min}(\vec{x}_i|t)$, whichever is larger. After a sufficiently large number of iterations, which is of the order of the size of the area of interest (scaling as $t^{2\zeta}$), all possible trajectories to endpoints within this area have been probed, and the barrier energies $B(\vec{x})$ do not change any more. The energy $B(\vec{x}_f)$ is then identified as the lower bound. Figure 10 shows the lower bound to the energy barrier for a line with the endpoint moving from the origin to sites within a distance of the order of t^ζ , for different values of t and averaged over 500 realizations of randomness. The distance $|\vec{x}_f - \vec{x}_i|$ has been scaled by t^ζ , and the energy by t^θ . After this rescaling, all the curves collapse, leading to the following scaling behavior for the lower bound,

$$\langle E_-(t, |\vec{x}_f - \vec{x}_i|) \rangle = t^\theta f_-(|\vec{x}_f - \vec{x}_i|/t^\zeta). \quad (10)$$

The function $f(y)$ should be proportional to $y^{\theta/\zeta}$ for small y . Again, for the simulated system sizes, this asymptotic scaling is not clearly seen. For $y > 1$, the scaling form in Eq.(10) breaks down since the minimal energy is then a function of the angle ($|\vec{x}|/t$). We conclude that the lower bound to the barrier scales in the same way as the fluctuations in minimal energy, and consequently the energy barrier increases at least as t^θ , leading to $\psi \geq \theta$. The distribution $P(E_-)$ of the lower bound energy for a fixed distance $|\vec{x}| \propto t^\zeta$ is shown in Fig.11. It

appears to be half-Gaussian with width proportional to t^ζ .

The result $\psi \geq \theta$ is not surprising if we note that an even simpler lower bound is given by $\max(E_{min}(\vec{x}_f|t) - E_{min}(\vec{x}_i|t), 0)$, which evidently scales as t^θ since the distribution function of minimal energies decays exponentially fast, i.e. has no power-law tails (see Fig.9). To make sure that the scaling of the lower bound found above is not dominated by the neighborhood of final configurations with particularly high energies, we repeated the above simulations by allowing only endpoints with minimal energies smaller than the initial energy. This corresponds to a situation where the endpoint of the line only moves to positions which are energetically more favorable. The results are shown in Fig.10 and again collapsed by the scaling form

$$\langle \tilde{E}_-(t, |\vec{x}_f - \vec{x}_i|) \rangle = t^\theta \tilde{f}_-(|\vec{x}_f - \vec{x}_i|/t^\zeta). \quad (11)$$

As in the previous case, the asymptotic scaling $\tilde{f}_-(y) \propto y^{\theta/\zeta}$ for small y cannot be clearly seen. The energy distribution of the lower bound is again a half-Gaussian of width proportional to t^ζ and looks similar to Fig.11.

The same scaling behavior is also found when instead of the optimal trajectory for the endpoint, the shortest trajectory (a straight line) is chosen. In this case, the mean of the barrier energy E_0 has the scaling form

$$\langle \tilde{E}_0(t, |\vec{x}_f - \vec{x}_i|) \rangle = t^\theta f_0(|\vec{x}_f - \vec{x}_i|/t^\zeta) \quad (12)$$

(see Fig.10), again with a half-Gaussian distribution of width proportional to t^ζ . This, of course, does not represent a lower bound to the true barrier, but it will be important for the determination of an upper bound below, and is therefore included here.

The result $\tilde{E}_- \propto t^\theta$ (Eq.(11)) can be explained from the exponential tails of the distribution of minimal energies: If we assume that the endpoint of the line moves only in valleys of particularly low energy, we can successively remove all sites with the largest minimal energy from the set of possible endpoints, until the connectivity over the distance t^ζ breaks down. The remaining endpoints form percolation clusters, and their density is given by the corresponding percolation threshold. (This is analogous to random resistor networks describing the hopping resistivity for strongly localized electrons. The resistance of the whole sample is governed by the critical resistor that makes the network percolate [21].) Since the occupied sites are correlated over the distances considered, the value for the threshold is different from the site percolation limit of 0.5 in an infinite triangular lattice with no correlation between occupied sites. But for the present purpose, it is sufficient to know that this threshold is finite, and that therefore a finite percentage of all sites are below threshold. Since the distribution of minimal energies decays rapidly, its tail cannot contain a finite percentage of all sites. We conclude that the threshold is within a distance of t^θ from the peak, and

therefore that the energy fluctuation on the percolation cluster, and consequently the lower bound for the barrier, are proportional to t^θ .

We now proceed to construct an upper bound to the energy barrier. To this purpose, we specify a sequence of elementary moves which take the line from its initial to final configuration. The only elementary move allowed is flipping a kink along the line. Thus the point (τ, \vec{x}) can be shifted to $(\tau, \vec{x} \pm \vec{e}_i)$, where $\pm \vec{e}_i$ are the six vectors which connect a vertex in the triangular lattice to its nearest neighbors within the same sublattice. The algorithm is similar to the one in 2 dimensions: First, we choose a sequence of endpoints connecting the initial to the final endpoint which is as short as possible. Then, we draw all the minimal paths leading to these endpoints, and attempt to move the line through them sequentially. If two consecutive minimal paths have nowhere a distance larger than 1 (measured in units of $|\vec{e}_i|$), we can choose a sequence of elementary moves such that at most two bonds of the line are not on one or the other minimal path, leading to a barrier of order 1 between the two. If the distance is larger than 1, we proceed essentially in the same way as in 2 dimensions, i.e. we consider the midway points $(t/2, \vec{x}_i)$ which connect both lines via the shortest possible trajectory $x_i(t/2)$ (if there are several possibilities, we choose one at random). For each of these points, we find two minimal segments of length $t/2$ connecting on one side to $(0, \vec{x})$ and on the other to either $(t, \vec{x}_1(t))$ or $(t, \vec{x}_2(t))$. Then we move the line by repeatedly moving segments of length $t/2$, etc.

The energy of a candidate barrier is then given by

$$\begin{aligned} & \langle E_c^{(3d)}(t, t^\zeta) \rangle \\ & \simeq \langle E_0(t, t^\zeta) \rangle (1 + 2((1/2)^\theta + (1/4)^\theta + \dots)) \\ & = \langle E_0(t, t^\zeta) \rangle (-1 + 2/(1 - (1/2)^\theta)) \\ & = 12.0 \dots \langle E_0(t, t^\zeta) \rangle. \end{aligned} \quad (13)$$

In principle, one should add correction terms similar to those in Eqs.2 and 7. However, these corrections are sub-leading with respect to t^θ and will be neglected.

As mentioned in section III, we cannot rule out that the energies of minimal segments are independent from each other. In the worst case, where they are completely dependent, Eq.(13) has to be multiplied by $\sqrt{\log_2 t}$. This may result in an additional factor proportional to $\sqrt{\ln t}$ in the upper bound, but does not otherwise affect any of our conclusions. The number of independent candidate barriers increases with some power in t . Since their energy distribution decays like a Gaussian, we can take their maximum in the same way as before, and we finally obtain the following estimate for the upper bound,

$$\begin{aligned} & E_+^{(3d)}(t, |\vec{x}_f - \vec{x}_i|) = \\ & = \langle E_c(|\vec{x}_f - \vec{x}_i|, t) \rangle + \sqrt{2 \ln N} \text{var} E_c(|\vec{x}_f - \vec{x}_i|, t) \\ & \simeq \left(\sqrt{\ln t} \right) t^\theta f_+(|\vec{x}_f - \vec{x}_i|/t^\zeta). \end{aligned} \quad (14)$$

We have thus shown that the energy barrier encountered by a FL moving in a $2d$ or $3d$ random medium has an upper and a lower bound which both increase as t^θ , except for logarithmic factors. It thus follows that the barrier itself scales as t^θ , confirming the hypothesis $\psi = \theta$. Since the arguments are mainly based on the exponential tails of the minimal energy distributions, it is expected that the result $\psi = \theta$ holds also in higher dimensions. The only requirement is that the tails in the distributions of minimal energies still decay sufficiently rapidly.

V. BARRIERS TO FAR FROM MINIMAL CONFIGURATIONS

In the previous sections, we discussed energy barriers which have to be overcome by a line moving between minimal energy configurations. We showed that such lines can stay in an energy interval $\langle E_{min} \rangle \pm \text{const } t^\theta$. However, a line may initially have an energy which is much larger. The initial configuration of a FL penetrating the system may be straight and parallel to the external magnetic field. If a system is cooled down from high temperatures, configurations of the FL are random walks of roughness exponent $\zeta = 1/2$. An initial configuration with roughness exponent $\zeta = 1$ is found for FLs driven close to a depinning transition [22]. If the temperature is low (as we always assume in this paper), the line then relaxes to some metastable state. The FL will ultimately reach a configuration of minimal energy, only if it is not separated from it by abnormally high barriers. We therefore show in this section that the line can reach the minimal energy region by going only over barriers which are not larger than order of t^θ . We specify an algorithm for moving a line of length $t = 2^m$ from any initial configuration to one of minimal energy. The algorithm is similar to that presented in the previous sections, and leads to barriers of the order of t^θ .

First, we assume that its initial roughness is not larger than that of minimal energy paths. Let $\{x_n(\tau)\}$ for $\tau = 0, \dots, t$ be the initial configuration of the line, and $\{x_0(\tau)\}$ a minimal energy configuration with $x_n(0) = x_0(0)$ and $x_n(t) = x_0(t)$. We then define a sequence of paths $\{x_m(\tau)\}$, $m = 1, \dots, n-1$, which are constrained to go through the points $x_n(kt/2^m)$ for $k = 0, 1, \dots, 2^m$ and are composed of 2^m minimal segments of length $t/2^m$. The energy of such a segment is smaller than the energy of any other piece of a path with larger m which has the same endpoints as the segment. We now move the line successively through this sequence of configurations, going from the largest to the smallest value of m . The configurations $\{x_{m+1}(\tau)\}$ and $\{x_m(\tau)\}$ intersect each other at the points $\tau = kt/2^m$, with $k = 0, \dots, 2^m$. We therefore can move the line from the configuration $\{x_{m+1}(\tau)\}$ to $\{x_m(\tau)\}$ by successively moving segments of length $t/2^m$. In many cases, the segments have to overcome a loop, and then we apply the algorithm defined previously.

In contrast to the previous sections, these loops do not separate two minimal configurations, but one minimal segment, and another constrained at its midpoint, a constellation which occurred also in the previous sections as an intermediate situation. Since we restricted the roughness of the initial configuration to less than that of minimal paths, the size of the loops does not exceed t^ζ . The number of independent candidate barriers within a loop is therefore smaller than, or equal to, $N_c \propto (2^m)^{\alpha'}$ from previous arguments, where the exponent α' depends on the model. The energy of each candidate path is smaller than, or equal to, the energy $E_c(2^m)$, which was also obtained in the previous sections. The total number of loops is less than or equal to $1 + 2 + \dots + 2^{n-1} < 2^n = t$, and the energy of each candidate barrier is certainly overestimated if we assume that all loops are of size t . We therefore find an upper bound to the barrier which is the maximum of $t t^{\alpha'} = t^{1+\alpha'}$ candidates chosen from a distribution $P(E_c(t))$ with $\langle E_c(t) \rangle \propto t^\theta$, and with a Gaussian tail. As we saw in section III, such a maximum scales as $t^\theta \sqrt{\ln t}$. We therefore have shown that a line can move from any configuration with roughness exponent less than ζ to a minimal energy configuration by crossing barriers which are not larger than order of t^θ , provided that the barriers between minimal configurations scale also as t^θ .

A similar result can be obtained for any initial configuration of the line. To demonstrate this, let us look at the configuration $x_t(\tau) = -\tau$, which is as far as possible from a minimal configuration. We then define a sequence of paths $\{x_m(\tau)\}$, for $m = t-2, t-4, \dots, 0$, with $x_m(\tau) = -\tau$ for $\tau \leq m$, and connecting the points $(m, -m)$ and $(t, -m)$ by a minimal path. To go from one configuration to the next one, the line has to overcome a loop of size no bigger than $(t-m)^\theta < t^\theta$. There are consequently proportional to $t^{1+\alpha'}$ candidates for barrier paths of length between 2 and t . We certainly find an upper bound to the barrier by assuming that all these candidates have the length t , and that their energies are taken from a (half-) Gaussian distribution of width proportional to t^θ . The upper bound consequently scales as $t^\theta \sqrt{\ln t}$.

VI. MULTIPLE BARRIERS

So far, we tacitly assumed that the activation barrier is given by the difference of the highest energy encountered by the line and its initial energy, just as in thermally activated chemical reactions. This assumption, however, has no solid foundation, since the line does not simply move over an isolated maximum, but through a random energy landscape. In addition, it is not at all clear how results obtained for a point-like particle in a 1-dimensional energy landscape can be generalized to lines moving in 2- or 3-dimensional systems. To shed some light at least on the first of these points, we study in this section a

particle in a 1-dimensional energy landscape at low temperatures. We tilt this landscape by a small angle to take into account the effect of an external driving force. Using the Fokker-Planck equation, we calculate the stationary particle current through this tilted energy landscape. We find that it is not the difference between the maximal and initial energies, but the difference between the maximal and the minimal energies, which determines the activation barrier.

The Fokker-Planck equation for the probability density $P(x, t)$ of an overdamped particle in one dimension is

$$\frac{\partial P}{\partial t} = \Gamma \frac{\partial}{\partial x} \left(kT \frac{\partial}{\partial x} + \frac{\partial V(x)}{\partial x} \right) P(x, t). \quad (15)$$

Here, Γ is the inverse of the product of the particle mass and the friction coefficient. The potential $V(x)$ is the sum of the random potential $V_B(x)$ and a driving term $-Fx$, where F is the constant driving force. Depending on the boundary conditions, this equation has different stationary solutions $\partial_t P = 0$. If the boundary is an infinitely high wall at both ends of the system, we obtain the equilibrium solution $P(x) \propto \exp(-V(x)/kT)$, and zero current

$$j = \Gamma \left(kT \frac{\partial}{\partial x} + \frac{\partial V(x)}{\partial x} \right) P(x, t) = 0.$$

We instead look for a solution where particles enter the system at one end and leave it at the other end. This solution is most readily found by assuming periodic boundary conditions, $P(L) = P(0)$ and $V_B(L) = V_B(0)$. This situation corresponds to a periodic energy landscape which has been tilted, and where each section of length L contains the same number of particles. Clearly, this leads to a stationary flow through the system, with particles entering a section at one end and leaving it at the other. In the limit of small driving force F , the stationary current is found by considering only terms up to linear order in F (order zero gives the equilibrium solution of the untilted system), and is given by [23]

$$j = \Gamma FL / \left[\int_0^L e^{-V_B/kT} dx \int_0^L e^{+V_B/kT} dx \right]. \quad (16)$$

In the limit $T \rightarrow 0$, the integrals are dominated by the neighborhoods of the maximum and the minimum of the potential, leading to $j \propto \exp[(V_B^{max} - V_B^{min})/kT]$. This means that the particle mobility is determined by the difference between the energy maximum and minimum. This result is plausible since the particles explore all of the energy landscape and therefore also go down to the valleys and have to come up all the way again [24].

Generalizing the above arguments to a line in 2 dimensions is difficult, and we did not succeed in solving the corresponding Fokker-Planck equation analytically. Evidently, the line can avoid configurations with particularly high energy, which seems to justify the assumption that

the barrier is the lowest possible which separates the initial and the final configurations. In the light of Eq.(16), however, we may need to define the barrier energy as the difference between the maximum and the minimum, instead of the difference between the maximum and the initial energy. If so, we should add to the barrier the difference between the initial energy and that of the absolute minimum along the trajectory of the line. We know, however, that the distribution of minimal energies has only exponential tails, and that therefore both types of barriers scale in the same way. Consequently, our results do not depend on the precise definition of the barrier. To confirm this, we plot in Fig.12 the scaling functions $\bar{g}_1^{(sr)}$ and $\bar{g}_1^{(lr)}$ for the barrier to 2-dimensional lines with either short-range or long-range correlated randomness, determining the difference between the maximal and minimal energy of all intermediate configurations of the line. It can clearly be seen that the barrier energy still satisfies Eqs.(4) and (8).

VII. CONCLUSIONS

In this paper we considered various properties of the energy landscape of one of the simplest realizations of glassy systems. We showed that, under fairly general conditions, the energy barriers encountered by a line descending into the region of minimal energies, or moving within this region, scale in the same way as the fluctuations in minimal energy. This means, in particular, that there exist no metastable configurations which cannot be left by going over energy barriers smaller than, or equal to, the fluctuations in minimal energy.

Similar arguments are applicable to interfaces in random media, like domain walls in 3-dimensional random bond and random field Ising models. When the interface moves from an initial to a final configuration, with part of its boundary fixed, a given boundary point moves along a line. For each position of this boundary point, there exists a configuration of minimal energy. The maximum of these minimal energies certainly is a lower bound to the barrier. If the distribution of minimal energies has no power-law tails, this lower bound scales in the same way as the minimal energy fluctuations. An upper bound can be constructed using a similar algorithm as for the line: Each time the interface (or a segment of it) has to overcome a loop, we bisect it and repeatedly move the upper and lower segment through a sequence of minimal configurations. In this way, the interface is always composed of minimal segments, and it should scale in the same way as the lower bound (except for logarithmic factors, and provided that the lower bound energy distribution has no power-law tails).

Given these results for lines and interfaces, it is likely that they generally hold for elastic media with impurities, e.g. for a bunch of flux lines. The latter situation is certainly of much more physical relevance than a single

FL. Our results for a single FL, may thus have provided a glimpse into the complexity of the energy landscape of more complicated glassy systems.

Based on results for particles in 1-dimensional energy landscapes, we also argue that the energy barrier should not be defined with respect to the initial energy, but to the minimal energy along the trajectory of the line. It stills remains a challenge to generalize this argument to lines in 2- or higher dimensional energy landscapes, and to find a more precise expression for the response of the line to a driving force, starting from the Fokker-Planck equation.

ACKNOWLEDGMENTS

This work started in collaboration with Lev Mikheev (see Ref. [10]). We have also benefitted from discussions with Alan Middleton, who has independently discovered many interesting results pertaining to energy barriers [25]. BD is supported by the Deutsche Forschungsgemeinschaft (DFG) under Contract No. Dr 300/1-1. MK acknowledges support from NSF grant number DMR-93-03667.

-
- [1] M. Kardar, *Lectures on Directed Paths in Random Media*, Les Houches Summer School on Fluctuating Geometries in Statistical Mechanics and Field Theory, August 1994 (to be published; see cond-mat/9411022).
 - [2] K. H. Fischer and J. A. Hertz, *Spin glasses*, Cambridge University Press, Cambridge (1991).
 - [3] J. A. Mydosh, *Spin glasses: an experimental introduction*, Taylor & Francis, London (1993).
 - [4] G. Blatter, M. V. Feigel'man, V. B. Geshkenbein, A. I. Larkin, and V. M. Vinokur, *Rev. Mod. Phys.* **66**, 1125 (1994).
 - [5] D. R. Nelson and V. M. Vinokur, *Phys. Rev. B* **48**, 13060 (1993).
 - [6] P. W. Anderson and Y. B. Kim, *Rev. Mod. Phys.* **36**, 39 (1964).
 - [7] D. S. Fisher, M. P. A. Fisher, and D. A. Huse, *Phys. Rev. B* **43**, 130 (1991).
 - [8] L. Ioffe and V. M. Vinokur, *J. Phys. C* **20**, 6149 (1987).
 - [9] D. A. Huse and C. L. Henley, *Phys. Rev. Lett.* **54**, 2708 (1985).
 - [10] L. V. Mikheev, B. Drossel, and M. Kardar, *Phys. Rev. Lett.* **75**, 1170 (1995).
 - [11] B. Drossel, *J. Stat. Phys.*, in press (1995).
 - [12] D. A. Huse, C. L. Henley, and D. S. Fisher, *Phys. Rev. Lett.* **55**, 2924 (1985).
 - [13] T. Hwa and D. S. Fisher, *Phys. Rev. B* **49**, 3136 (1994).
 - [14] L. V. Mikheev, preprint (1994).
 - [15] J. Galambos, *The Asymptotic Theory of Extreme Order Statistics* (John Wiley & Sons, New York, 1978).

- [16] M. Kardar, J. Appl. Phys. **61**, 3601 (1987).
- [17] E. Medina, T. Hwa, M. Kardar, and Y.-C. Zhang, Phys. Rev. A **39**, 3053 (1989).
- [18] J. G. Amar and F. Family, Phys. Rev. A **41**, 3399 (1990).
- [19] J. M. Kim, A. J. Bray, and M. A. Moore, Phys. Rev. A **44**, 2345 (1991).
- [20] T. Halpin-Healy, Phys. Rev. A **44**, R3415 (1991).
- [21] V. Ambegaokar, B. I. Halperin, and J. S. Langer, Phys. Rev. B **4**, 2612 (1971).
- [22] M. D. Ertas and M. Kardar, Phys. Rev. Lett. **73**, 1703 (1994).
- [23] H. Risken, *The Fokker-Planck equation*, Springer-Verlag, Heidelberg (1984), Eq.(11.45).
- [24] More general discussions of the motion of a particle in a one-dimensional energy landscape can be found in S. Scheidl, Z. Phys. B **97**, 345 (1995); and in P. Le Doussal and V. M. Vinokur, to be published.
- [25] A. Middleton, unpublished.

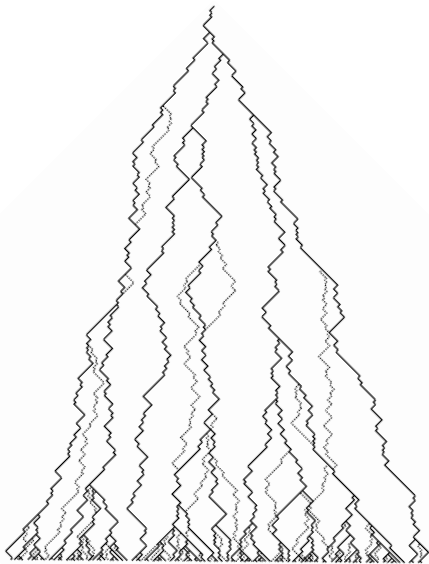


FIG. 1. Minimal paths of length $t = 256$ for a FL in 2 dimensions to endpoints between $x = -96$ and $x = +96$ (solid), and the barrier paths between them (dotted).

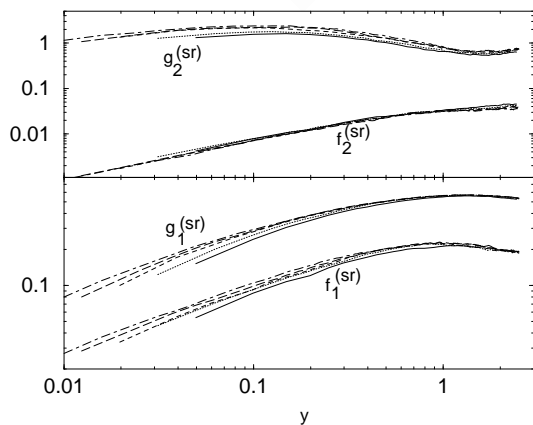


FIG. 2. Scaling functions $f_1^{(sr)}(y)$, $f_2^{(sr)}(y)$, $g_1^{(sr)}(y)$, and $g_2^{(sr)}(y)$ (see Eqs.(1), (4), and (5)) for the mean and variance of the lower and upper bounds; averaged over 2000 realizations of randomness, for $t = 256$ (solid), 512 (dotted), 1024 (dashed), 2048 (long dashed), and 4096 (dot-dashed).

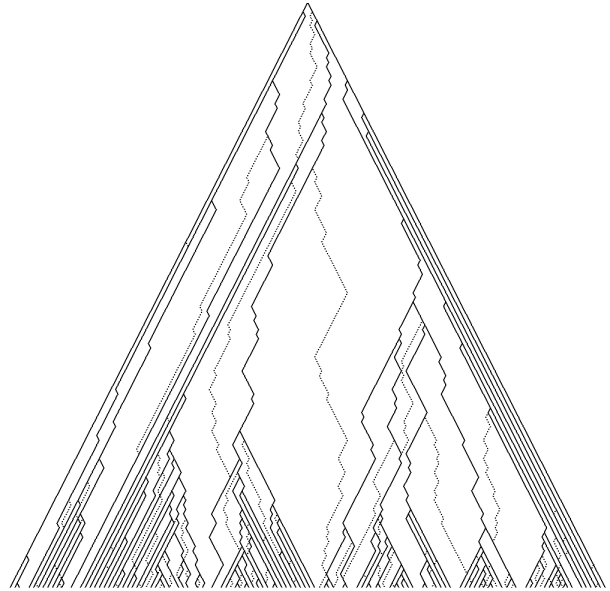


FIG. 3. Minimal paths of length $t = 128$ to endpoints between $x = -t$ and $x = +t$ (solid), and the barrier paths between them (dotted), in the random-field Ising model.

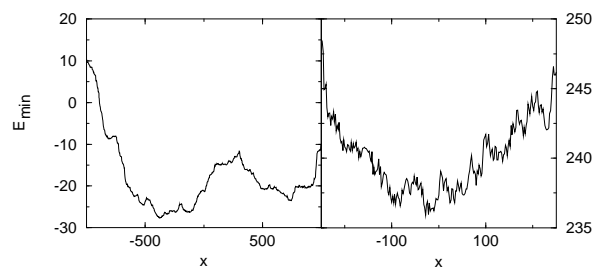


FIG. 4. The minimal energy E_{min} as function of the endpoint position x for $t = 1024$ and (a) long-range correlated randomness, (b) short-range correlated randomness.

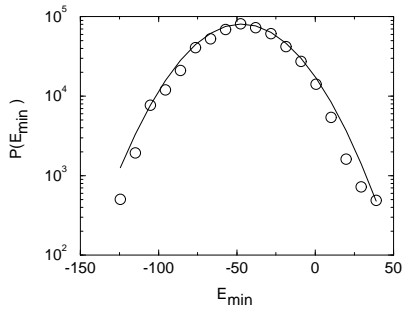


FIG. 5. The distribution $P(E_{min})$ of minimal energies for $t = 1024$ and long-range correlated randomness. The solid line is a Gaussian distribution; deviations from it indicate a third cumulant.

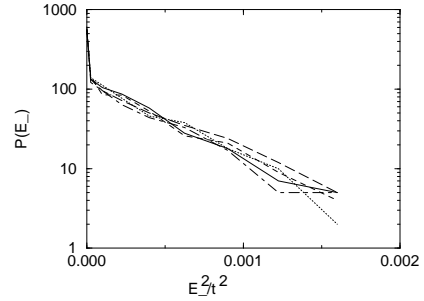


FIG. 7. Distribution of minimal energy for an Ising domain wall in 2 dimensions with random fields. The symbols are the same as in the previous figure.

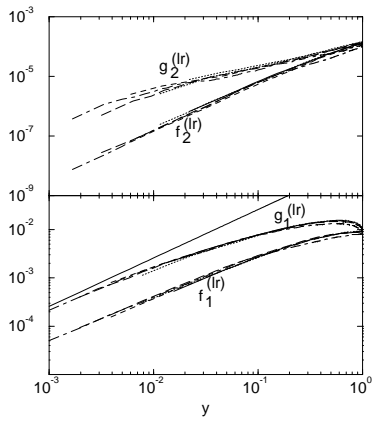


FIG. 6. Scaling functions $f_1^{(lr)}(y)$, $f_2^{(lr)}(y)$, $g_1^{(lr)}(y)$, and $g_2^{(lr)}(y)$ (see Eqs.(6), (8), and (9)) for the mean and variance of the lower and upper bounds; averaged over 1000 realizations of randomness, for $t = 256$ (solid), $t=512$ (dotted), 1024 (dashed), and 2048 (long dashed). The straight line has the slope 1.

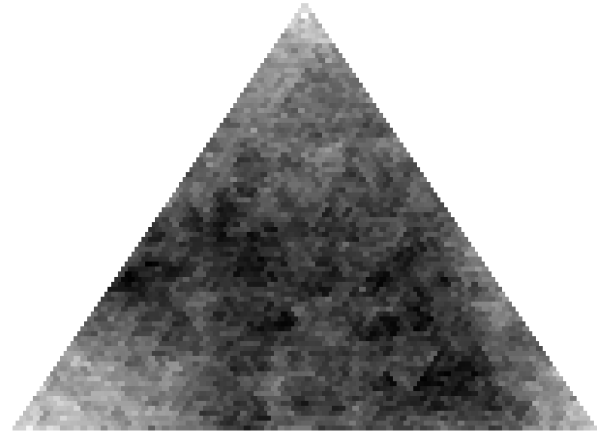


FIG. 8. Minimal energies of paths of length $t = 288$ in 3 dimensions to endpoints \vec{x} with $|\vec{x}| < O(t^\epsilon)$. The higher energies are indicated by white shading, and the lower energies by darker shades.

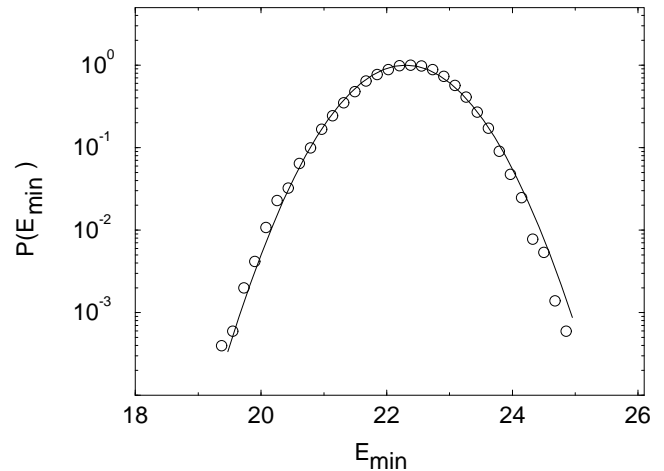


FIG. 9. Probability distribution $P(E_{min})$ of minimal energies $E_{min}(\vec{0}|144)$ in 3 dimensions, averaged over 50,000 realizations of randomness. The solid line is a Gaussian distribution.

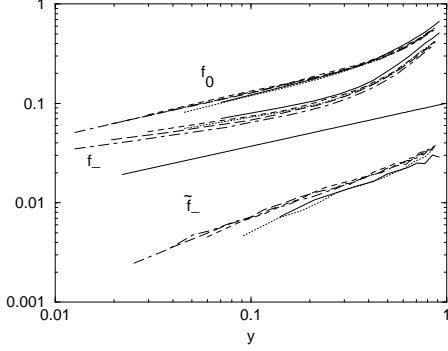


FIG. 10. Scaling functions $f_-(y)$, $\tilde{f}_-(y)$, and $f_0(y)$ defined in Eqs. (10)–(12) for $t = 72$ (solid), 144 (dotted), 288 (dashed), 576 (long dashed), and 1152 (dot-dashed), averaged over 500 realizations of randomness. The straight line has slope $\theta/\zeta = 0.39$.

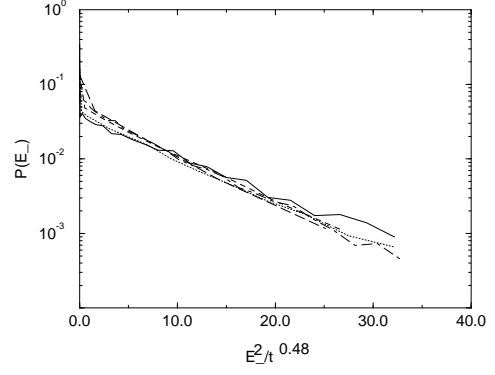


FIG. 11. Probability distribution of E_- . The parameters and symbols are the same as in Fig.10.

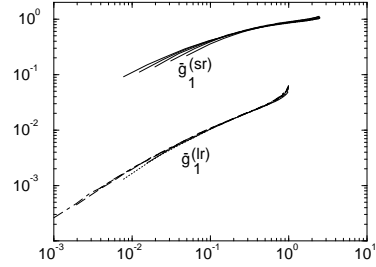


FIG. 12. Scaling functions $\bar{g}_1^{(sr)}(y)$ and $\bar{g}_1^{(lr)}(y)$, similar to $g_1^{(sr)}(y)$ in eq.(4) and $g_1^{(lr)}(y)$ in eq.(8), but with the barrier definition of section VI.